Volume 61
Number 24
25 March 2025
Pages 4577–4728

ChemComm

Chemical Communications

rsc.li/chemcomm

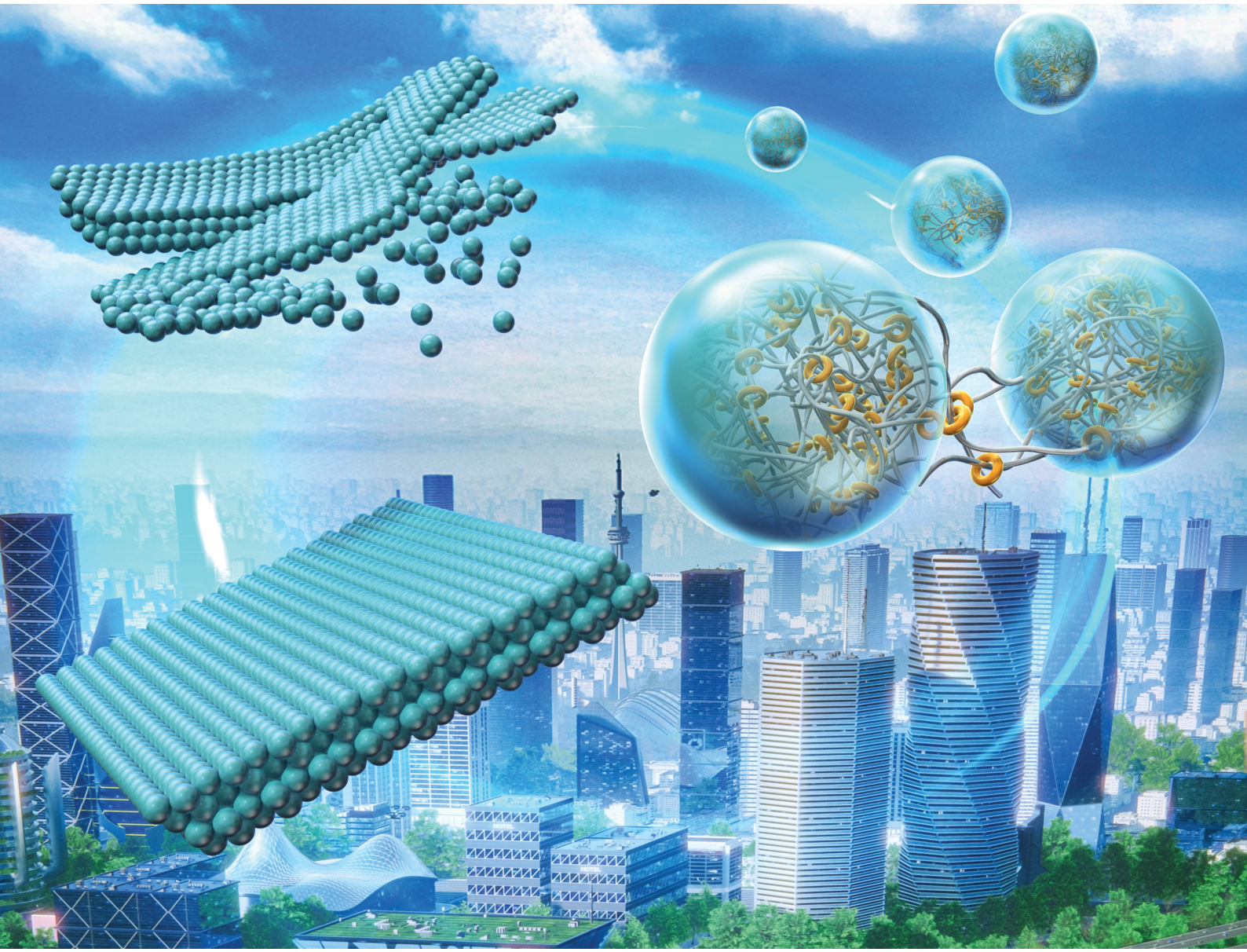

ISSN 1359-7345

ROYAL SOCIETY OF CHEMISTRY

FEATURE ARTICLE

Yuma Sasaki, Daisuke Suzuki *et al.*

Nano/microparticle-based tough and recyclable polymers toward a sustainable society

ChemComm

FEATURE ARTICLE

View Article Online
View Journal | View Issue

Cite this: *Chem. Commun.*, 2025, **61**, 4606

Nano/microparticle-based tough and recyclable polymers toward a sustainable society

Yuma Sasaki, *[ab] Yuichiro Nishizawa, [a] Takuma Kureha [c] and Daisuke Suzuki *[a]

Received 29th January 2025,
Accepted 3rd February 2025

DOI: 10.1039/d5cc00543d

rsc.li/chemcomm

By virtue of their unique properties, polymer nano/microparticles constitute important building blocks for the construction of functional nanomaterials. Although intense research efforts in this field have laid the foundation for the applications of polymer nano/microparticle-based latex films, cutting-edge innovations in the recycling of polymer materials are still required for the realization of a sustainable society. This feature article reviews our recent attempts to develop the applications of polymer nano/microparticles in the context of a circular society on the basis of the precise synthesis of single nano/microparticles and multiscale structural analysis.

1. Introduction

1.1 Polymer nano/microparticles

Polymer nano/microparticles with sizes ranging from several dozens of nanometers to several micrometers are generally used in dispersions in solvents such as water, forming colloids that may function both as single particles in a medium and also as particle assemblies. The properties of single particles and their latexes depend on the structural characteristics of the polymer particles, including size, shape, hydrophilicity/hydrophobicity, charge, crosslinking density, and molecular weight. To obtain the desired functions, these properties must be precisely controlled during the particle-synthesis stage.[1–6] Polymer nano/microparticles have excellent long-term stability in storage due to their high dispersion stability. Moreover, their high specific surface area has been exploited to develop biomedical transporters and catalysts and pharmaceutical coatings, since polymer nano/microparticles can be synthesized using only water.[7–11] The mechanical properties of single particles have also been attracting attention; in particular, tuning their size and uniformity as well as controlling their conductivity as a function of the contact area with a substrate, the elastic modulus, and the ability to recover when unloaded have enabled their use as spacers for electronic components. In addition, assembling polymer nano/microparticles allows expanding the functions of polymer colloids from the nano/microscopic to the macroscopic scale. For instance, colloidal crystals exhibit structure-dependent colors.[12–14] Moreover, polymer nano/microparticle assemblies exhibit fast responsiveness to stimuli compared with other bulk materials given that their stimuli-response rate is proportional to the square of the particle size.[15,16]

1.2 Nano/microparticle-based (latex) films: film-formation mechanism

Dispersions of nano/microparticle-based materials may form continuous films upon drying, which are generally called latex. Here, we mainly focus on synthetic elastomer latex films prepared by drying aqueous dispersions or by means of a few simple reactions. Recent progress on natural latex composed of poly(*cis*-1,4-isoprene) has already been discussed elsewhere.[17] Owing to their simple and cost-effective process, synthetic polymer latexes are used in applications such as paintings,[18,19] inks,[20–22] adhesives,[23] and strain-responsive devices,[24,25] with a global production of 55 million tons per year.[26] However, despite the current attempts to reduce the use of volatile organic compounds, which are harmful to humans and the environment,[27] replacing solvent-based latexes with waterborne latexes is challenging because the mechanical properties of waterborne latex films are usually inferior to those of polymer bulk materials.

Therefore, substantial efforts have been devoted to improving the physical and chemical stability of nano/microparticle-based materials for enhanced film formability, mechanical properties, and durability against external stimuli (*e.g.*, UV, ozone, and solvents). It should be noted here that especially film formation is strongly linked to most film properties. Generally, the film-formation process proceeds as follows: (i) polymer nano/microparticles dispersed in water are packed during the drying process. (ii) If the glass-transition temperature (T_g) of the polymer that forms the nano/microparticle is lower than the environmental

[a] *Graduate School of Environmental, Life, Natural Science and Technology, Okayama University, 3-1-1 Tsushimanaka, Kita-ku, Okayama, Okayama 700-8530, Japan. E-mail: pz2r6it2@s.okayama-u.ac.jp, d_suzuki@okayama-u.ac.jp*
[b] *Graduate School of Textile Science & Technology, Shinshu University, 3-15-1 Tokida, Ueda, Nagano 386-8567, Japan*
[c] *Department of Frontier Materials Chemistry, Graduate School of Science and Technology, Hirosaki University, 3 Bunkyo-cho, Hirosaki, Aomori 036-8561, Japan*

temperature, the nano/microparticles can deform and coalesce owing to the increase in capillary force[28,29] and osmotic pressure.[30] (iii) After water is completely removed, polymer-chain diffusion allows the interface between particles to be spanned, which leads to the formation of continuous polymer films.[31–33] Most of the basic research on the formation of latex films was reported until the early 2000s, including several exhaustive reviews.[34–36] On the basis of these studies, the minimum film-forming temperature (MFFT), which is the lowest temperature at which the dispersion can form a mechanically coherent film, and which is strongly related to the mechanical properties, is often used as an indicator of film formability. In general, low MFFT values below the T_g of the polymer that forms the nano/microparticles are conducive to film formability.

1.3 Nano/microparticle-based (latex) films: mechanical properties

According to the film-formation process mentioned above, increasing the coalescence strength of the particles and reducing the MFFT are key factors for improving the mechanical properties and film stability. For details on the film-formation ability, the reader may direct his/her attention to the excellent review by Aguirre *et al.*[37] Although the mechanical properties of waterborne latex films are considered to be weaker than those of organic-solvent-cast films, few reports have directly compared both cases. Meanwhile, several studies have focused on the difference in mechanical properties between latex and bulk systems. For instance, continuous films of hard particles such as poly(methyl methacrylate) particles prepared *via* organic-solvent casting have been proven to be mechanically tougher than those prepared using aqueous latex systems,[38] which was attributed to the higher mobility of the polymer chains in organic solvents compared to that in aqueous systems, resulting in more continuous polymer networks. Furthermore, latex films obtained from aqueous dispersions have shown a lower quantum efficiency of energy transfer than tetrahydrofuran-cast films, indicating that the polymer chains cannot fully entangle between individual nano/microparticles in aqueous media.[39] It is generally accepted that latex films prepared *via* simple drying are brittle owing to insufficient polymer-chain entanglement, and increasing the toughness of latex films constitutes an active area of research as shown in Table 1.

1.3.1 Improving the mechanical properties of latex films by promoting coalescence (Table 1)

(i) Thermal annealing. Thermal annealing above the T_g of the polymers that form nano/microparticles has been often used to improve the mechanical properties of latex films by promoting the polymer interdiffusion between nano/microparticles. Fujii *et al.* have investigated the effect of thermal annealing on the tensile strength and elongation of latex films.[40] Atomic-force-microscopy (AFM) height images have revealed that the film surface becomes smooth after thermal annealing due to the coalescence of polymer particles. Hiroshige *et al.* have found that annealing at high temperatures results in tougher films owing to higher particle deformation compared to that upon annealing at lower temperatures.[41] Therefore, the final film structure depends on the initial state of particle deformability. Meanwhile, Zosel and Ley have revealed that intraparticle crosslinking suppresses the polymer interdiffusion across the microparticle surface.[42] These findings later became the basis for a theoretical interface-adhesion-strength model developed using the scaling rule by Aradian *et al.*[43] These studies suggest that the mechanical properties of waterborne latex films can be increased when the polymer chains are fully interdiffused across the boundaries of nano/microparticles *via* thermal annealing in a manner similar to that of the bulk state. However, the mechanical properties of the resulting films have not yet reached those of bulk systems. Fujii *et al.* have suggested that the presence of residues such as surfactants and inorganic salts hinders reaching the mechanical strength and elongation of the bulk state.[40]

(ii) Plasticization. Plasticizers, which are widely used in industry, also promote the diffusion between particles by increasing the affinity between polymer particles or between polymer chains and solvent molecules. This promotion of the particle coalescence often results in a MFFT that is by more than 10 °C lower than the T_g,[50,51] which contributes to the softening of films and an increase in mechanical strength or elongation. However, plasticizers generally contain volatile organic solvents, leading to safety concerns during film formation. Therefore, introducing hydrophilic functional groups to use water as the plasticizer has emerged as an attractive approach.[52] Hydrophilic organic acids such as acrylic acid form high-strength bonds with substrates by virtue of the polarity of the carboxyl groups and are used as the main ingredients in adhesives. An investigation of the tensile strength of latex films composed of copolymers of organic acids and elastomers revealed an improvement in the mechanical properties.[53] Although hydrogen bonds have been suggested to contribute to film toughening, the specific toughening mechanisms are not fully understood owing to the complex factors originating from plasticization and bonding.

(iii) Latex blends or core–shell structures. The formation of a latex blend of high-T_g particles and low-T_g particles is the simplest technique to reduce the MFFT and tune the elastic modulus of latex films.[54] However, blending sometimes results in segregation if there is no special treatment. To solve this problem, the synthesis of core–shell particles has been developed to enhance the coalescence of nano/microparticles. Core–shell nano/microparticles are synthesized *via* semicontinuous emulsion polymerization or seeded emulsion polymerization. Although the MFFT can be reduced by the soft shell,[55] controlling the particle morphology remains difficult because it depends on the interfacial energy between polymers or between the polymer and the solvent. Thus, attention should be paid to identifying undesirable structures such as secondary particles using microscopy techniques including transmission electron microscopy (TEM).[56] Moreover, the introduction of a hard phase often leads to an increase in the hardness or modulus of films but a decrease in elongation at break.[57]

1.3.2 Improving the mechanical properties of latex films by strengthening interparticle interactions

(i) Interparticle covalent crosslinking (ICC). In contrast to the method of lowering the MFFT by promoting the interdiffusion

Table 1 Comparison between the toughening methods for latex films

Toughening methods (discoveries)	Synthesis	Analytical techniques	Effects on mechanical and other stabilities	Limitations	Ref.
Thermal annealing (1950s)	Thermal treatment of films above their T_g	Microscopy; scattering; dynamic mechanical analysis; fluorescence energy transfer; tensile tests	Improved elongation, mechanical strength; hardening	High energy required	40–44 45 and 46 47 and 48 49
Solvent-based plasticization (1950s)	Addition of plasticizers compatible with both solvent and polymers	Microscopy; MFFT measurements	Improved elongation; softening	Emission of harmful volatile organic solvents	50 and 51
Hydro-plasticization (1980s)	Copolymerization with hydrophilic monomers	Differential scanning calorimetry; MFFT measurements	Improved elongation; softening	Poor water resistance	52 and 53
Blending hard/soft particles (1980s)	Blending of low- and high-T_g polymer-particle dispersions	MFFT measurements; tensile tests; dynamic mechanical analysis	Improved elongation or mechanical strength	Inhomogeneous structure (*e.g.*, segregation)	54
Core (hard)–shell (soft) articles (1960s)	Emulsion polymerization in the presence of polymer particles; mixing with homopolymer emulsions	Microscopy; MFFT measurements; tensile tests	Improved elongation or mechanical strength	Complicated synthesis; undesirable by-products	55–58
Core (soft)–shell (hard) particles (2010s)	Emulsion polymerization in the presence of polymer particles; Pickering miniemulsion polymerization	Microscopy; MFFT measurements; tensile tests	Improved elongation and mechanical strength; hardening	Complicated synthesis; prone to crack formation	37, 59 and 60
Interparticle covalent crosslinking (1980s)	1. Introduction of reactive functional groups on particles; 2. chemical post-reaction	Solvent-extraction to calculate gel contents; swelling tests; spectroscopy; tensile tests	Improved mechanical strength; hardening; high solvent resistance; low hysteresis loss	Difficult to control crosslinking rate; harmful residues; reduced elongation	61–63
Interparticle non-covalent crosslinking (1950s)	Copolymerization with carboxylic acids/multiple hydrogen-bonding monomers	Spectroscopy; swelling tests; tensile tests	Improved mechanical strength; hardening; high solvent resistance; self-healable	Special synthesis; poor coalescence	53 and 64–67
Composites with fillers (1980s)	Mixing of inorganic fillers with polymer particle dispersions	Microscopy; dynamic mechanical analysis; tensile tests	Improved mechanical strength; hardening	Inhomogeneous structure; poor coalescence; increased brittleness	59 and 68–71
Intraparticle rotaxane crosslinking (2017)	Mini-emulsion polymerization in the presence of rotaxane crosslinkers	Microscopy; scattering; tensile and tear tests	Improved elongation and mechanical strength	Special rotaxane synthesis; universality of rotaxane unknown	49, 72 and 73
Poly(methyl acrylate) nano/microparticles (2023)	Emulsion polymerization of methyl acrylate	Microscopy; scattering; simulations; tensile tests	High elongation and mechanical strength	Universality of chemical structure unknown	74–76 77

of nano/microparticles, chemical crosslinking of the particle surface can effectively increase the strength of latex films. Generally, the particle surfaces are chemically modified with carboxy groups, vinyl groups, or other reaction sites and then crosslinked using dehydration–condensation reactions with acetoacetate or diacetone, epoxy groups, the reaction between hydroxy groups and melamine, or silane-coupling reactions. Details on the different curing reactions are provided elsewhere.[61,62] The introduction of covalent bonds between nano/microparticles can improve the durability against a variety of stimuli, especially water and organic solvents; however, these curing reactions sometimes use organic solvents and highly toxic reagents such as isocyanates or reagents with low water solubility. Therefore, thermally induced self-crosslinking reactions such as those involving *N*-methylolacrylamide have been proposed as an alternative without using additives.[63] In general, the effect of interparticle covalent crosslinking (ICC) on the mechanical properties of latex films follows the same trend as that of bulk elastomers, *i.e.*, the increase in the number of covalent bonds in the polymer network results in an increase in modulus and a decrease in elongation.

(ii) Interparticle noncovalent crosslinking. The interparticle chemical crosslinking mentioned above requires the fine tuning of crosslinking post-reactions depending on the diffusion and reaction kinetics, leading in some cases to brittle films. To avoid complex procedures and problems, monomers containing multiple hydrogen bonds, such as urea or ureidopyrimidinone, that form strong intermolecular interactions[78] have been developed and introduced into nano/microparticles, endowing

them with solvent resistance and self-healing properties.[64] Recent progress on the chemical and physical properties using supramolecular interactions have been summarized in a recent perspective article.[65] Bio-based tannic acid[66] can also strengthen the interparticle interactions mainly formed *via* hydrogen bonding. Despite reaching high strength, the interdiffusion of polymer chains between particles is hindered by high bonding energies. Recently, physical bonding based on ionic interactions in the presence of both anionic and cationic functional groups has been introduced.[67] To suppress the coagulation of particles, a particle steric stabilizer is added. As a general trend, the ionic or hydrogen bonding introduced at the interface of particles is often reorganized after debonding, which increases hysteresis (loss of reversibility).

(iii) Fillers. Fillers such as calcium carbonate,[68] colloidal silica,[69] polymers,[70] and cellulose nanocrystals[59] have been used to strengthen the interparticle interactions. As these fillers do not deform themselves under external mechanical stimuli, the accumulation of stress at the polymer matrix around the fillers is thought to contribute to the increase in modulus.

In contrast with the number of papers describing strategies to improve the mechanical properties of latex films, the origin of the mechanical properties has not yet been elucidated. As Aguirre *et al.* have pointed out in their recent perspective article on film formability,[37] solving the paradox of using additives to increase the toughness of latex films remains to be addressed. Efficient methods to improve the mechanical properties of waterborne latex films still remain to be developed. To understand the mechanical properties of latex films, a comprehensive understanding of their structure is required.

1.4 Recycling of polymer materials

Improving the mechanical properties of materials, including latex films, can contribute to their long-term durability. Meanwhile, appropriate processing and recycling strategies are important. The global accumulation of polymer materials from their use between 1950 and 2017 has been estimated to be 9.2 trillion tons[79] and is expected to keep increasing. According to the United Nations Environment Program, the effective recyclability of polymer materials is still insufficient, with a global recycling ratio of 14% in 2020.[80] In addition, several million tons per year of plastic waste are floating in rivers and oceans.[81] Accordingly, the development of bio-based and biodegradable plastics is essential,[82] albeit hindered by (i) preparation costs, (ii) limited structures, and (iii) low versatility.

Hence, the realization of a sustainable society requires improving the recycling techniques. Recycling methods are broadly classified into closed-loop and open-loop recycling.[83,84] In closed-loop recycling, recycled materials exhibit the same properties as the original ones. Recycled materials can be used in the same applications as the original material. In open-loop recycling, recycled materials have different properties from the original material and are used to manufacture entirely new products. Recycling techniques are then further classified into mechanical, chemical, physical, and biological recycling as well as energy recovery, depending on the recycling approach used to recover plastic material, raw material (*e.g.*, monomers), or energy. Especially in these areas, closed-loop recycling is essential for a circular economy because closed-loop recycling helps to stably secure valuable resources and reduce the environmental burden. Recently, by introducing degradation points into small units, *i.e.*, monomers or oligomers, of polyethylene, true closed-loop recycling has been achieved.[85] However, in addition to cost, energy, and processing limitations, some additives or mixtures must be removed from materials before recycling. Closed-loop recycling without conversion to monomers or oligomers is mainly limited to polyethylene terephthalate (PET), which is mechanically cut to flakes or pellets and then converted to PET resin. Further research in this regard is required to address issues such as costs.

In summary, toward a circular economy, the main strategies are improving the mechanical properties of latex films to enhance their long-term durability and recycling. This feature article summarizes methods to obtain mechanically tough nanoparticle-based films without using additives (Fig. 1). Our first attempt was based on using molecular machines in nano/microparticles by introducing a rotaxane crosslinker (RC) as the key component. We also succeeded in obtaining a poly(methyl acrylate) (pMA) nano/microparticle-based film that was as tough (>50 MJ m^{-3}) without any additives. The following sections describe the synthesis of nanoparticles that form tough films and the elucidation of the mechanisms from a mesoscale analysis using microscopy to the atomic scale using simulations. The final section introduces the concept of nano/microparticle-based materials recycling, which differs from that of conventional recycling methods.

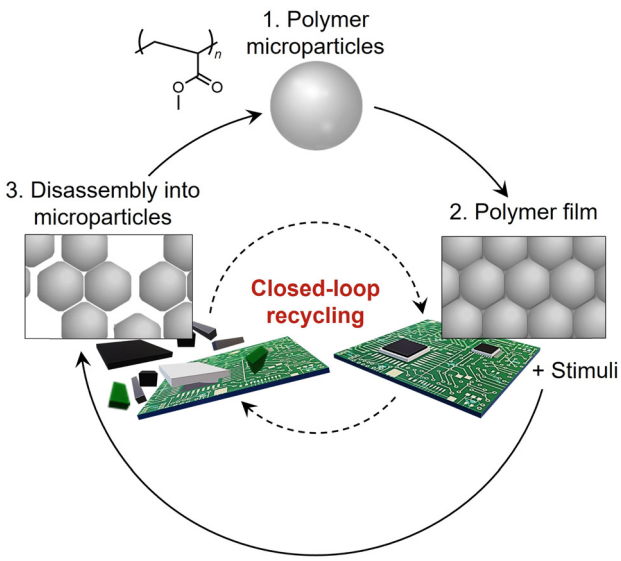

Fig. 1 Concept of nano/microparticle-based materials recycling. Adapted from ref. 75 with permission from the Royal Society of Chemistry (copyright 2023 Royal Society of Chemistry).

2. Tough nano/microparticle-based films

The toughening of bulk polymer materials has been achieved using various methods, such as inducing the dissipation of stress at stress-concentrated points by constructing double-network structures, introducing fillers, or forming supramolecular interactions.[86] Polymers have also been crosslinked using rotaxanes to induce toughening.[87] Takata *et al.* have synthesized a well-defined [2]RC in which a crown-ether wheel is interlocked with an alkyl or polyester wheel,[88–90] finding that the high steric demand of the axle[91] and the topology[92] (*i.e.*, the number of components) affects the mechanical properties. Recently, the shuttling motion of the axle has been demonstrated *via* mechanochromic luminescence.[93] However, the specific effect of the RC on the improvement of the mechanical properties remains unclear, and further work is required to extend the scope of the toughening strategy using RCs in various chemical species. In this context, we wondered whether rotaxanes would affect the mechanical properties of nano/microparticle-based films. First, we evaluated the introduction of rotaxane crosslinking points in a single nano/microparticle (Fig. 2(a)). The following section describes our studies on the effect of RCs on the mechanical properties in comparison with conventional chemical crosslinkers.

2.1 Preparation of rotaxane-crosslinked nanoparticles

The detailed synthesis of the RC that we used (Fig. 2(c)) has been reported by Sawada *et al.*[89] This molecule is difficult to introduce into nano/microparticles by conventional emulsion polymerization due to its high hydrophobicity.[72] Therefore, we focused on the mini-emulsion polymerization method, which has been developed by Ugelstad to incorporate hydrophobic molecules.[72,73,94–96] To incorporate RCs into single polymer nano/microparticles, a water-insoluble RC was introduced into acrylate-monomer (*e.g.*, alkyl (meth)acylate) droplets with a nanoparticle scale of ~100 nm. Upon adding a water-soluble initiator such as sodium peroxodisulfate, water-soluble radicals enter the monomer droplets and initiate the polymerization (Fig. 2(c)). After the polymerization is terminated, the monomer droplets are converted into nano/microparticles crosslinked by the RCs that have reacted in the droplet.

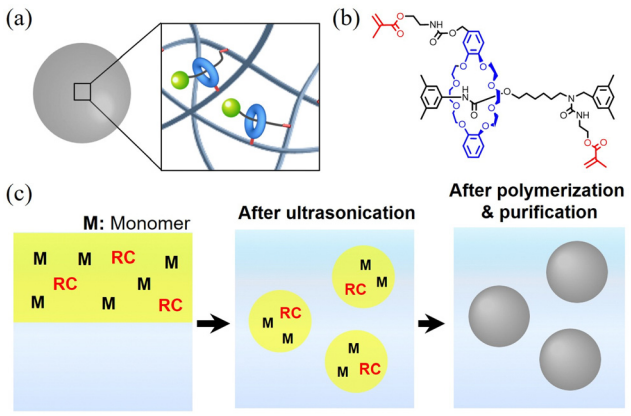

Fig. 2 (a) Schematic illustration of a rotaxane-crosslinked nano/microparticles. (b) Chemical structure of the rotaxane crosslinker. (c) Schematic illustration of the synthesis of rotaxane-crosslinked nanoparticles polymerized from fined monomer droplets. Adapted with permission from ref. 72 (copyright 2017 John Wiley & Sons) and ref. 73 (copyright 2023 American Chemical Society).

2.2 Characterization of isolated polymer nano/microparticles

To understand the properties and functions of latex films, it is crucial to gain insight into the structure and properties of their constituent particles. However, the characterization of single nano/microparticles is difficult because aggregates are easily formed due to capillary forces when using simple drying methods. This is not the case when elastomer nano/microparticles are adsorbed at the air–water interface and then transferred onto a solid substrate. Thus, single particles can be arranged at intervals without aggregation, thereby enabling their observation (Fig. 3(a)).[97] For instance, AFM measurements revealed that the height of the nano/microparticles increased with increasing crosslinker feed ratio, suggesting that the formation of crosslinking points results in harder nano/microparticles (Fig. 3(b)).[73–75]

2.3 Effect of rotaxanes on the mechanical properties of nanoparticle-based films

A nanoparticle-based film was formed by drying a dispersion, which provided a colorless thin film because the T_g of the constituent poly(butyl acrylate-*co*-methyl methacrylate) (14 °C) is slightly below that of the environmental temperature (25 °C) (Fig. 4(a)). The mechanical properties of nano/microparticle-based films were initially evaluated using uniaxial tensile tests. Hiroshige *et al.* found that nanoparticle films of rotaxane-crosslinked poly(butyl acrylate-*co*-methyl methacrylate), a versatile

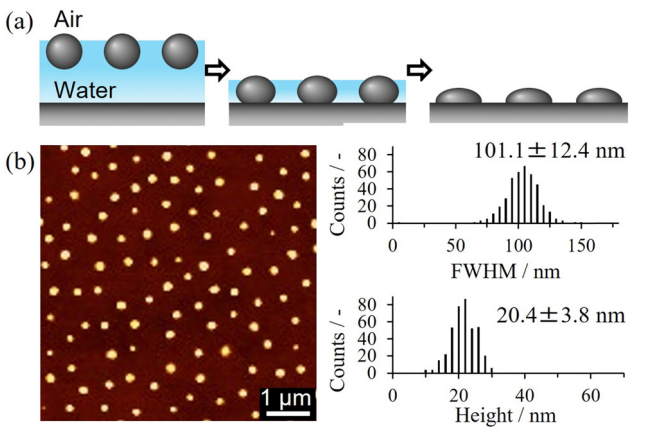

Fig. 3 (a) Schematic illustration of soft nano/microparticles adsorbed at the air–water interface. After drying, the particles are arranged at intervals. (b) AFM image of nanoparticles dried on a glass substrate arranged at intervals. Particle size (full width at half maximum, FWHM) and height distributions. Adapted with permission from ref. 73 (copyright 2023 American Chemical Society) and ref. 97 (copyright 2021 Royal Society of Chemistry).

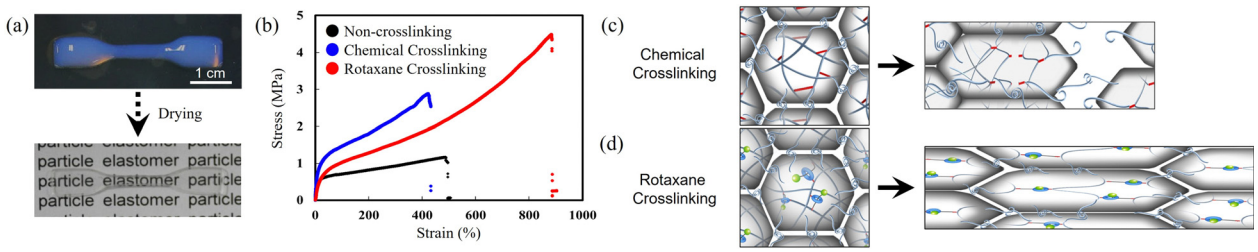

Fig. 4 (a) Photographs before and after formation of a nano/microparticle-based film. (b) Stress–strain curves of films composed of polymer nanoparticles crosslinked with rotaxanes or chemical crosslinkers. (c) and (d) Schematic illustration of plausible fracture mechanisms of (c) chemically crosslinked and (d) rotaxane-crosslinked nano/microparticle-based films. Adapted with permission from ref. 72 (copyright 2017 John Wiley & Sons).

acrylic elastomer, were more stretchable than non-crosslinked or chemically crosslinked nanoparticles (Fig. 4(b)).[72] As shown in Fig. 4(c), for nanoparticle-based films, stress concentrates on the chemical crosslinking points under elongation and polymer interdiffusions across nano/microparticles are hindered by inter-particle crosslinking. Thus, the polymer chain can easily slip from the particle interface, which has been associated with fracture events. On the other hand, the polymer interdiffusion across the nano/microparticles are not suppressed compared to chemical crosslinking due to the flexibility of the crosslinking structure (*cf.* Section 3.3). In addition, rotaxane crosslinking in nano/microparticles has been linked to the dissipation of stress at the crosslinking points by the sliding motion of the RC in each nanoparticle (Fig. 4(d)). This work provided a new approach for toughening, circumventing the limitations of conventional methods in terms of the simultaneous improvement of elongation and mechanical strength.

Expanding the RC effect to various kinds of polymers and diverse deformation modes is important for the practical application of RCs. For instance, tearing was found to cause not only uniaxial elongation but also unique toughness. The introduction of RCs into the nano/microparticles of poly(ethyl acrylate-*co*-methyl methacrylate) nano/microparticle-based films resulted in a simultaneous increase in elongation and mechanical strength upon uniaxial stretching, as an example of expansion of chemical species. The investigation of the crack-propagation behavior from the initial notch in the specimen revealed that the crack started to propagate in the direction perpendicular to the initial notch (Fig. 5(a)).[73] Conversely, non-crosslinked or chemically crosslinked nano/microparticle-based films exhibited the generally observed tearing behavior, *i.e.*, the crack propagated in the direction parallel to the initial notch, indicating that rotaxane crosslinking is a key factor for the toughness against tearing. This is the first example of blunted crack propagation in polymer nano/microparticles, which is conventionally observed in anisotropic bulk elastomers or gels constructed by fiber or filler reinforcement, strain-induced crystallization, and phase separation. Furthermore, the toughness originating from blunted tearing depends on the degree of crosslinking in nano/microparticles in a wide elongation speed range (Fig. 5(b)). This result indicates that particle deformation is important for toughness and blunted crack propagation. Although the mechanism of the blunted

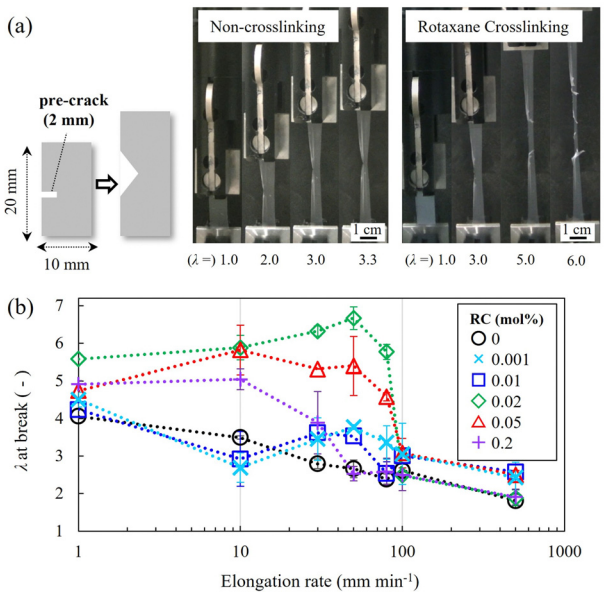

Fig. 5 (a) Crack propagation of a non-crosslinked and a rotaxane-crosslinked nanoparticle-based film during tear tests. (b) Elongation-rate dependence of the extension ratio (λ) at the break point for rotaxane-crosslinked nanoparticle-based films. Adapted with permission from ref. 73 (copyright 2023 American Chemical Society).

crack propagation is not yet fully understood, particle deformation during crack propagation seems to be the key factor for toughening (*cf.* Section 3.2; our attempts to visualize the deformed nano/microparticles).

2.4 Tough pMA nano/microparticle films

Recently, we have discovered that tough pMA particle-based films can be stretched with high elongation and mechanical strength, even without using rotaxanes (Fig. 6(a)).[75] Owing to the relatively high T_g of pMA ($\sim$10 °C) compared to that required for rubbers or adhesives, pMA has less applications than poly(butyl acrylate), whose T_g is much lower. To the best of our knowledge, reports on latex films composed of pMA homopolymer are scarce. In a uniaxial tensile test, pMA showed a fracture energy as an indicator of toughness of 67.3 MJ m^{-3}, which is equivalent to that of natural rubber (Fig. 6(b)). The fact that the mechanical strength of pMA nano/microparticle-based films is higher than that of the corresponding pMA bulk film

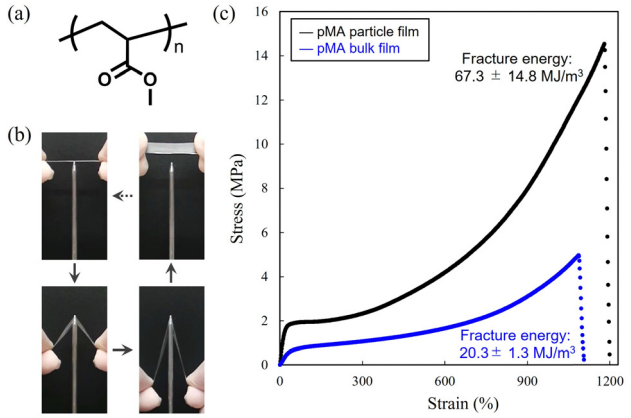

Fig. 6 (a) Chemical structure of poly(methyl acrylate) (pMA). (b) Snapshots of a pMA nano/microparticle-based film pierced by a sharp stick. (c) Stress–strain curves of a pMA nano/microparticle-based film and a pMA bulk film. Adapted with permission from ref. 75 (copyright 2023 Royal Society of Chemistry).

prepared *via* bulk polymerization with a chemical crosslinker (0.1 mol%) indicates that tough films can be prepared even from synthetic aqueous polymer particles without additives. In the following section, the toughening mechanisms elucidated *via* a structural analysis on the nanoscale are introduced.

3. Elucidation of the toughening mechanism *via* multiscale structural analysis

Given that the mechanical properties and functions of latex films strongly depend on the structure and properties of the nano/microparticles, intense research efforts have been devoted to the structural analysis of nano/microparticles. First, the nano/microparticles in latex films have been visualized using electron microscopy and AFM (*cf.* Section 1.3); however, the relationship between the nano/microparticle structure in terms of the packing state or deformability and the mechanical properties is difficult to ascertain. This is mainly due to the inherent difficulty in the characterization of single nano/microparticles (*cf.* Section 1.2) and the inhomogeneity of colloidal arrays. In this section, the visualization of nanoparticle-based films and the correlation between the film structure revealed by multiscale analysis and the mechanical properties are discussed.

3.1 Structural macroscopic analysis

Cracks and voids are the main cause of film breakage under elongation and can be easily detected by the naked eye or optical microscopy. The formation of uniform and stable particle-based films free of cracks is difficult due to the complexity of the systems, which are subjected to perturbations such as capillary force, inner stress, and convection in the case of aqueous systems. By performing a structural evaluation ranging from macroscopic observation using the naked eye to the nanoscale using AFM, Goehring *et al.* found that controlling

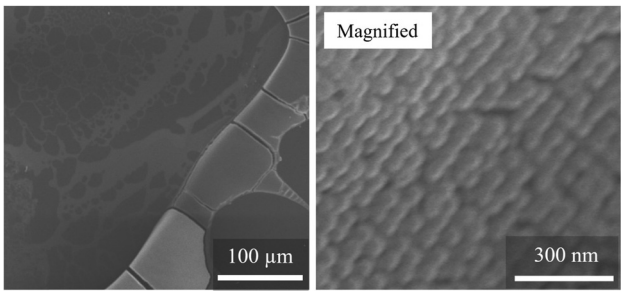

Fig. 7 SEM images of a nano/microparticle-based film showing cracks and voids. Adapted with permission from ref. 41 (copyright 2024 Springer Nature).

the drying speed and the elasticity of single nano/microparticles is important to obtain crack-free colloidal films.[98] Recently, beam-bending tests have been used to measure the stress developed during film formation, which is the main cause of crack evolution in such films.[60] To evaluate the physical and chemical properties of latex films, the formation of crack-free and locally independent structured films is desirable. Since the macroscopic structures also affect the reproducibility of mechanical tests, it is recommended to identify the presence of cracks using the naked eye or microscopy techniques such as optical microscopy and electron microscopy confocal laser scanning microscopy (CLSM) (Fig. 7).

3.2 Nanostructural analysis *via* AFM

AFM is a powerful tool for imaging the superficial nano/microstructure of latex films with high spatial resolution. The first structural analysis of a latex film using AFM was performed in 1992 by Wang *et al.* to investigate the structural changes caused by thermal annealing.[44] Subsequently, by smoothing the topographical images of the latex film surface obtained *via* AFM, the diffusivity of polymer chains, which changes due to thermal annealing and polymer crosslinking, and the effects of additives such as surfactants and coalescing aids, have been discussed.[99] Furthermore, using the force–distance curves obtained *via* cantilever indentation, the local mechanical properties of the film surface can be measured, including Young's modulus, stiffness, and viscoelasticity. This allows the identification of mixtures with different mechanical properties, such as inorganic fillers and polymer matrices. Indeed, stiffness mapping obtained from AFM revealed both the distribution of the composite material on the film surface and an increase in nanoscale mechanical properties that correlate with the macroscopic mechanical properties (*i.e.*, surface tack and hardness).[71]

Although the investigation of latex films using AFM is well-established, the AFM methods specifically tailored to the field of biology have only been introduced in the 2000s. Ando *et al.* have developed high-speed AFM (HS-AFM) with high time resolution (50 ms per flame) for observations in the liquid state, which has opened the door for an evaluation of the dynamic behavior of biomolecules such as proteins.[100,101] We have used this technique to evaluate for the first time artificial polymer microspheres, clarifying their dynamic behavior in

water.[102–108] The corresponding details are discussed elsewhere.[109] Recently, by optimizing the HS-AFM system for observations in air, the real-time observation of the surface structure of latex films has become possible, enabling the investigation of the structure of the surface and cross-section of nano/microparticle-based films over a large area as a movie (Fig. 8(a)).[75] To clarify the relationship between mechanical strength and the particle arrangement, an AFM instrument was equipped with a uniaxial-elongation device that contained a load cell. Observation of a pMA nano/microparticle-based film under stretching revealed that with increasing elongation ratio, the microparticles constituting the film deformed, while an increase in Young's modulus of the surface similar to the change in load applied to the film was observed (Fig. 8(b)). In particular, the nano/microparticles started to deform at the initial stage of elongation, where the load applied to the film increased (Fig. 8(c)). As the space between particles increased, the increase in the load applied to the film became smaller (Fig. 8(c)), indicating that a pull-out of the polymer chains between nano/microparticles occurred (Fig. 8(c)).[76] The change in stress of nano/microparticle-based films was found to correlate with the particle deformation. However, further investigations into the film structure under elongation have to consider structural features such as the inhomogeneity of particle arrays in order to clarify the toughening mechanism. Furthermore, although AFM is a powerful tool to directly visualize the structure and mechanical properties, it cannot depict the inner structure of films. Therefore, AFM should be combined with other analytical methods that can visualize the three-dimensional structure of films, such as CLSM. We have recently reported two-dimensional particle-based films and the characterization of their mechanical properties and particle alignment structure using AFM (*cf.* Section 4.2).

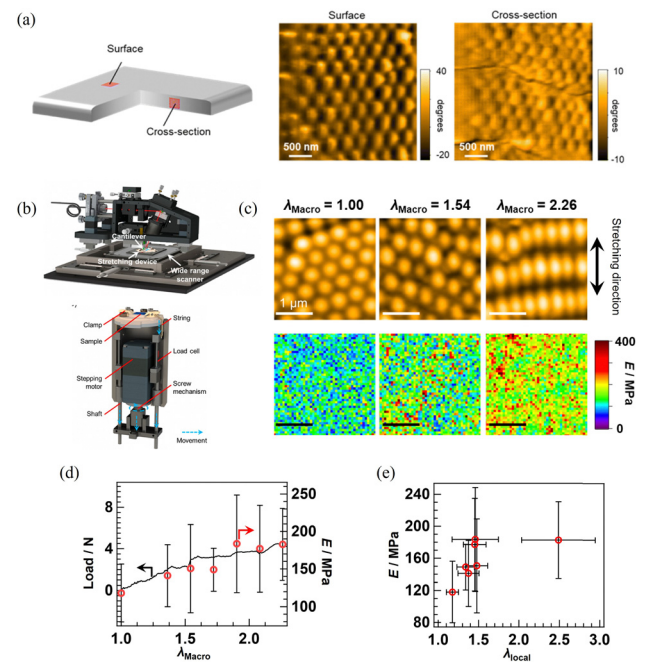

Fig. 8 (a) Phase images of the surface and cross-section of a pMA microparticle-based film obtained *via* HS-AFM observation (2 s per frame). (b) Schematic illustration of a tip-scan HS-AFM equipped with a uniaxial stretching device. (c) Height images and Young's modulus (E) mapping images of the pMA nano/microparticle-based film surface under elongation. (b) Load detected by load cell and averaged E as a function of the film elongation ratio (λ_{Macro}). (e) Relationship between averaged E and local deformation ratio (λ_{local}) calculated from the height image. Adapted with permission from ref. 75 (copyright 2023 Royal Society of Chemistry) and ref. 76 (copyright 2024 American Chemical Society).

3.3 Nanostructural analysis *via* scattering techniques

The nanostructures of latex films are mainly characterized by small-angle neutron or X-ray scattering (SANS/SAXS) and fluorescent energy-transfer measurements. These techniques have been applied primarily to quantify the interdiffusion between adjacent particles that occur on the nanometer scale. In 1986, Hahn *et al.* found that the radius of gyration (R_g) of deuterated nano/microparticles increases with increasing temperature and time of thermal annealing, confirming the occurrence of interdiffusion of polymer chains during the fusion of polymer particles after drying (*i.e.*, the third process in film formation).[110] Although particle interdiffusion had previously been evaluated mainly *via* electron microscopy, the use of scattering methods has enabled the quantitative evaluation of the degree of interdiffusion of polymer chains by ensemble averaging over the entire film. Furthermore, Linne *et al.* studied the penetration depth at the particle–particle interface by subtracting the R_g of the hydrogenated particles embedded in the deuterated particles from the R_g of the particles dispersed in solvents. Knowing the penetration depth is required to obtain sufficient mechanical strength (bending toughness and tensile strength) using hot-pressed molded deuterated polystyrene particles.[111]

In addition to SANS analysis, fluorescence techniques have been applied to characterize the structures of latex films, as *e.g.*, reported by Winnik *et al.*[45,112] Particularly, fluorescence-energy-transfer experiments allowed obtaining information on the polymer diffusion across the particle–particle (or polymer–polymer) interface using two latexes labeled with donor and acceptor dyes. The direct nonradiative energy transfer is applied to obtain the diffusion coefficient of the polymers on the particle surfaces, which helps understanding the film-formation mechanism.[46,113–116] Moreover, the effective length of the interfacial contacts between polymers where the energy transfer occurs (δ_{ET}) can be calculated.[113] SAXS measurements have also been applied to characterize latex films, in particular the colloidal particle ordering and crystalline structure. Dingenouts *et al.* have studied the packing of hard latex particles such as poly(methyl methacrylate) and polystyrene in the first step of film formation by analyzing the structure factor.[117] They concluded that the order achieved when these latexes are dried is closely related to the polydispersity of the system. Men *et al.* have investigated the colloidal crystalline structures of soft latex films consisting of poly(styrene-*co*-butadiene) particles with a T_g of ~5 °C.[118] Generally, soft latexes with low T_g form colloid crystals with a face-centered-cubic (fcc) lattice, whose

characterization provides information about the packing structure of the films.[47,119–122]

One of the greatest advantages of using scattering methods is that the structure during deformation can be studied at the nanoscale by attaching uniaxially elongated units. In 1996, Rharbi *et al.* reported the first investigation of the structure of a latex film during deformation.[58] They found that macroscopic deformation of the film occurred at the nanoscale. Subsequently, using synchrotron ultra-small-angle X-ray scattering, Men *et al.* discovered that nonaffine deformation also occurred with increasing stretching rates.[48,118]

As described above, we have developed tough nano/microparticle-based films consisting of rotaxanes-crosslinked microparticles, which can be formed without using additives and organic solvents.[49,72,73] Thus, they are suitable as models for scattering analyzes to investigate the relationship between the toughness and nanostructures. By applying this model, Kureha *et al.* have assessed other SAXS approaches to characterize the nanostructures related to interdiffusion between particles.[49] This analysis does not require deuterium or fluorescent labeling to obtain ensemble information of the inner nanostructure of particle films.[49] To quantify the depth of mixing of polymer chains with neighboring particles, together with the information obtained in the low-q region, they proposed the thickness of particle interfaces (t_{int}) as an indicator of the mixing of polymer chains (Fig. 9(a) and (b)).[41,49,73] As scanning electron microscopy (SEM) could not confirm the presence of mesoscopic voids on the surface of rotaxane-crosslinked nanoparticle-based films, which would influence the fracture behavior, especially the crack propagation, SAXS was performed using the beamlines of large synchrotron-radiation facilities (SPring-8 and Photon Factory in Japan) to investigate the nanoscopic structure. To clarify the toughness of nanoparticle-based films, the effect of rotaxane crosslinking on the film nanostructure was investigated.[73] In the scattering intensity ($I(q)$) and scattering vector (q) profiles in the low-q region for a non-crosslinked nanoparticle-based film, peaks originating from fcc colloidal crystals were observed, suggesting the presence of nanoparticles in the film. Meanwhile, in the case of a rotaxane-crosslinked nanoparticle-based film, the fcc colloidal peak almost disappeared at low RC concentration. In contrast, the appearance of an fcc peak in the low-q region suggested the presence of highly crosslinked nanoparticles. These results indicate the occurrence of strong deformation and the coalescence of nanoparticles.

Although the particle morphology and nanostructure can be observed using microscopy, they are virtually undetected in scattering measurements. This indicates that in pMA nano/microparticle-based films and other polyacrylate-based rotaxane-crosslinked films, the polymer chains deeply interpenetrate between the nano/microparticles, which would lead to high mechanical toughness. Combined with the result that the mechanical strength and elongation of pMA nano/microparticle-based films were higher than those of bulk pMA films prepared from photo-initiated polymerization,[75] it is feasible to assume that the particle–particle interface is almost negligible and cannot be considered as a mechanical weakness of particle-based films. Recently, Fujimoto *et al.*[74] have applied a novel all-atom molecular-dynamic (AA-MD) simulation for the first time to construct a crosslinked polymer nanoparticle with a diameter of ~16 nm and 580 monomer units using a chemical crosslinker (Fig. 10(a)).

Also, they discovered a low-density region near the microparticle surface, where the density is lower than that of the core. Moreover, the particle-surface region became narrower in the case of highly crosslinked nanoparticles, and the polymer density on the particle surface was higher than that of lowly crosslinked nanoparticles (Fig. 10(b)). This result supports the suppression of

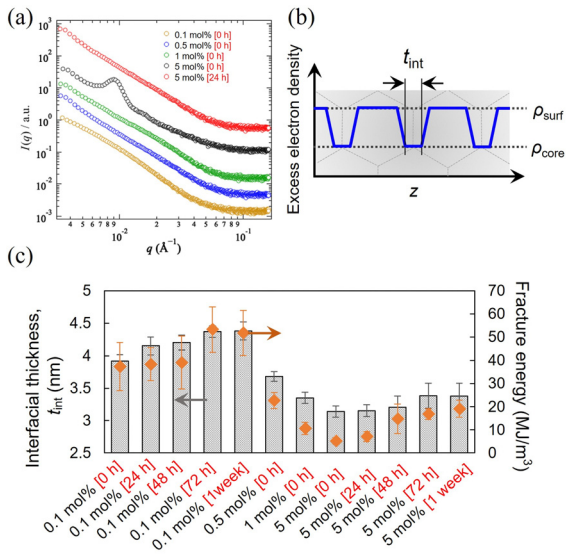

Fig. 9 (a) SAXS profiles of pMA-particle-based films. For a clear visualization, each scattering profile is offset vertically. (b) Schematic illustration of the distribution of the charge density on the particle surface; t_{int} is the thickness at which gradual changes in charge density occurs. (c) Visualization of t_{int} and the fracture energy of films composed of pMA nano/microparticles for various annealing times and crosslinker concentrations. Samples of the pMA nano/microparticle-based films are denoted as *X* mol% [*Y*], where *X* and *Y* indicate the crosslinker amount fed during the polymerization and the annealing time (0 h, 24 h, 48 h, 72 h, 1 week), respectively. Adapted with permission from ref. 75 (copyright 2021 Royal Society of Chemistry).

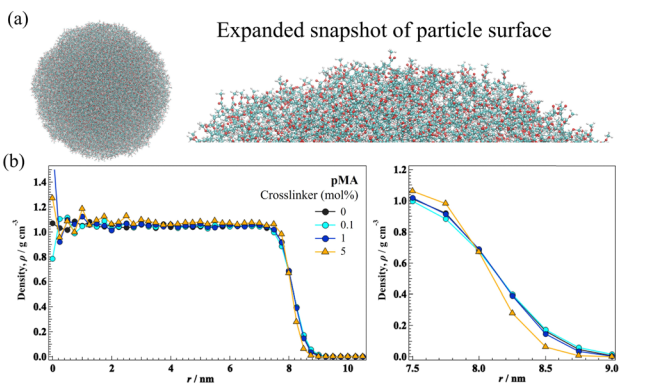

Fig. 10 (a) Left: A pMA nanoparticle prepared using AA-MD simulations. Right: Magnified picture. The cyan, red, and white spheres represent C, O, and H atoms, respectively. (b) Density profile obtained from AA-MD simulations as a function of the distance from the particle center (radius) at 480 K. Adapted with permission from ref. 74 (copyright 2024 American Chemical Society).

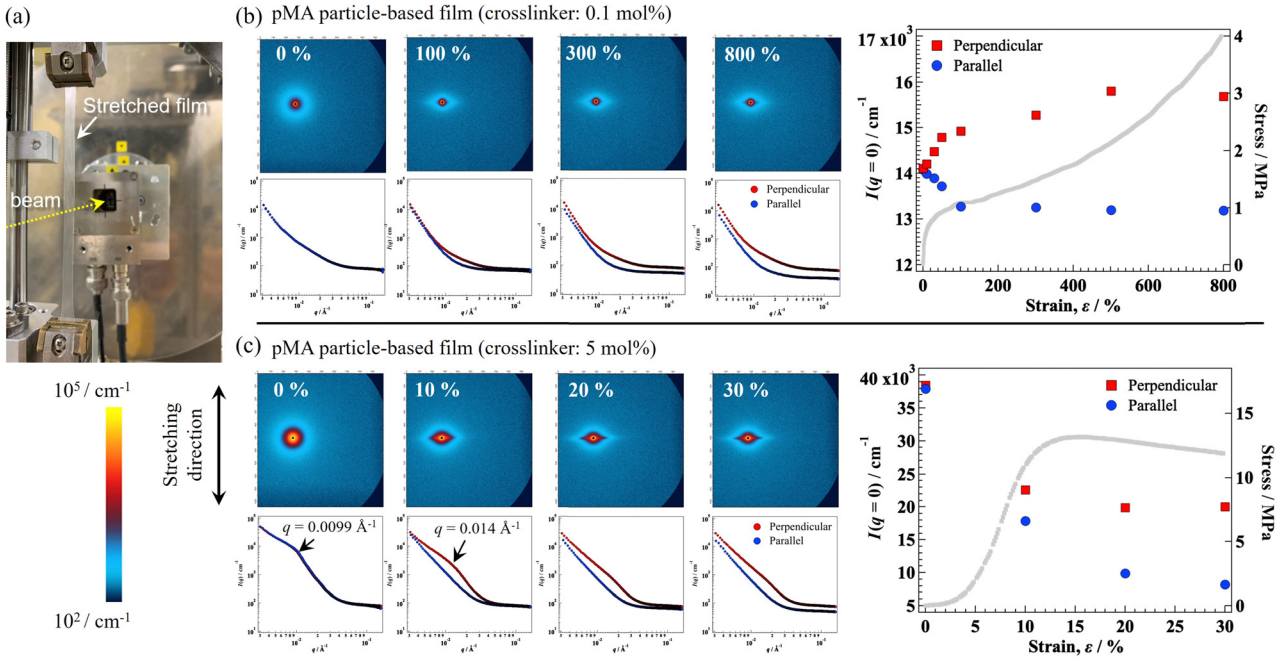

Fig. 11 (a) Photograph of a stretched film in the SAXS device. Two-dimensional SAXS patterns and one-dimensional scattering intensities under elongation of (b) lowly crosslinked and (c) highly crosslinked pMA nano/microparticle-based films under elongation. The color scale of the scattering pattern is the same for both films. Forward scattering intensities for the parallel or perpendicular direction relative to that of the elongation of (b) lowly crosslinked or (c) highly crosslinked pMA nano/microparticle-based films. Adapted with permission from ref. 74 (copyright 2024 American Chemical Society).

interdiffusion of highly crosslinked nanoparticles suggested by SAXS. These multiscale nanostructural analyzes will provide deeper insights into the fracture behavior of nanoparticles.

For further clarification of the structural changes occurring under elongation, SAXS was performed by Namba *et al.* on the fixed-state of elongated films.[74] They revealed that, at the initial stage of elongation (strain up to ~100%), the intensity in the direction perpendicular ($I_{(0,pend)}$) to the stretching steeply increased, indicating particle deformation (Fig. 11(a)). Upon further elongation (strain >100%), $I_{(0,pend)}$ slowly increased, indicating that the area of interdiffusion at the particle interface increased (Fig. 11(b)). In this region, under elongation, the contribution of the slip motion of the pMA chains also increased. Moreover, the change in intensity correlated well with the mechanical stress under elongation (Fig. 11(c)). According to these studies, the unique deformation mode originating from the particle assembly can be attributed to the mechanical properties of the nanoparticle films.

4. Elucidation of the toughening mechanism: microparticle compression in the two-dimensional state

In this article, we have focused on latex films formed by drying a particle-containing dispersion, which are regarded as three-dimensional colloidal assemblies characterized by a complex structure due to the presence of defects such as voids. Consequently, the analysis of the particle structures in the height direction is challenging. Considering that generating a particle assembly on a two-dimensional plate could help evaluate the mechanical properties in relation to the packing structure and deformed state of the nano/microparticles, we adopted Langmuir–Blodgett (LB) techniques to form a two-dimensional colloidal assembly. Colloidal nano/microparticles adsorbed at the air–water or oil–water interface act as surfactants. Soft particles have lower adsorption energy than rigid particles as the latter have a larger contact area on account of their deformability. For example, hydrogel microparticles, which are swollen by water and highly deformed in aqueous media, can be used as stabilizers of bubbles or emulsions using their softness.[123] Furthermore, the stability of the water–air(oil) interface can be tuned by the particle packing state or adsorbed state of the hydrogel microparticles. Thus, the correlation between the packing structure of hydrogel microparticles at the air–water interface and the mechanical properties of the hydrogel microparticle assembly has attracted much research attention.[124,125] However, in these studies, since the mechanical properties were estimated from the relation between surface pressure (π) and surface area (A), the mechanism of the dynamic deformation of a hydrogel microparticle at the air–water interface against external mechanical stress and the effect of an individual hydrogel microparticle on the mechanical properties of a hydrogel microparticle assembly remained unclear. In this section, the direct visualization of hydrogel microparticles under deformation is discussed.

4.1 Visualization of microparticle deformation

To visualize a hydrogel microparticle array at the air–water interface, a fluorescence microscope was attached to the Langmuir trough (Fig. 12(a)). Direct visualization of the air–water interface revealed that although most hydrogel microparticles

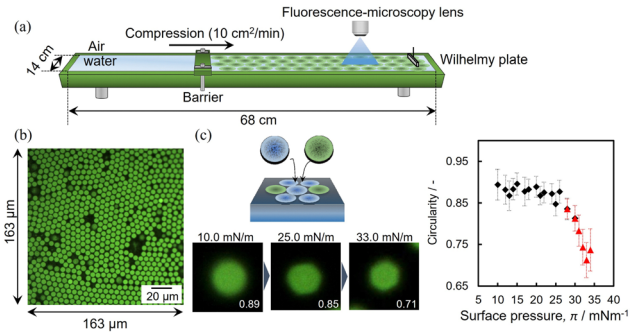

Fig. 12 (a) Schematic illustration of the Langmuir–Blodgett method. To visualize single hydrogel nano/microparticles, the particles were fluorescence-labeled. (b) Fluorescence microscopy images of single hydrogel microparticles at different surface pressures. (c) Deformation of a single microparticle in terms of the degree of deviation from circularity as a function of surface pressure. Adapted with permission from ref. 127 (copyright 2024 Royal Society of Chemistry).

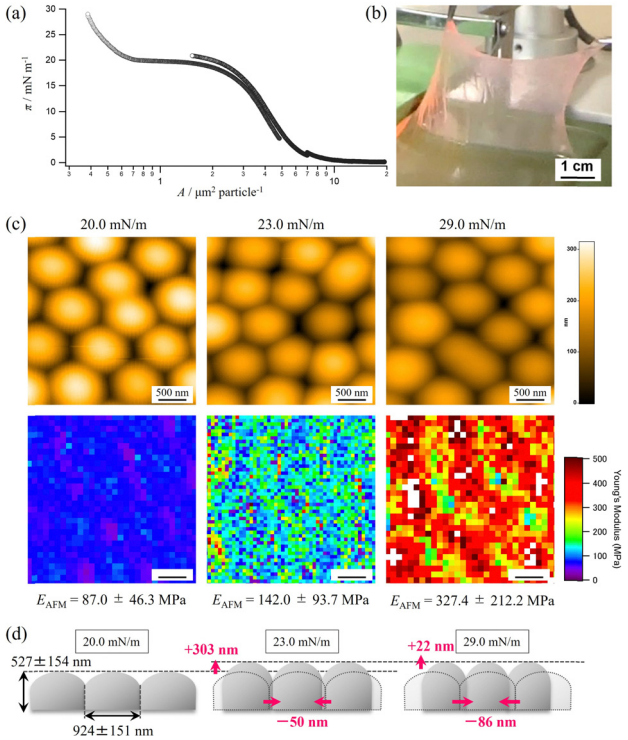

Fig. 13 (a) π and area per particle (*A*) isotherm of pMA microparticles adsorbed at the air–water interface. (b) Photograph of a monolayer particle film taken at high π (29 mN m^{-1}). (c) HS-AFM height images and Young's-modulus mapping of a pMA monolayer particle film with different π. NND and E_{AFM} refer to the nearest neighboring distance between microparticles and average Young's modulus of the film surface in the range of 20 μm × 20 μm, respectively. (d) Schematic illustration of the structural change in compressed pMA particles analyzed *via* AFM. Adapted with permission from ref. 77 (copyright 2024 John Wiley & Sons).

were aligned and closely packed, some defects and voids were observed (Fig. 12(b)). Kawamoto *et al.* have discussed the physical properties (*e.g.*, surface pressure and compression modulus) of a two-dimensional Langmuir film at the air–water interface between particle–particle contacts in the compressed state.[126] However, the effect of the deformation of the hydrogel microparticle on the compression behavior remained unclear. Then, micron-sized hydrogel microparticles that were sufficiently large for visualization were synthesized. Using these large hydrogel microparticles, individual hydrogel microparticles were clearly distinguished by mixing non-fluorescent-labeled hydrogel microparticles (Fig. 12(c)),[127] revealing that the hydrogel microparticles were deformed from their originally circular shape upon increasing the surface pressure by the compression of microparticles at the air–water interface. Considering the latex-film-formation process, particle deformation, and interdiffusion of polymer chains at the particle–particle interface, the alignment of particles is important to obtain microparticle-based films. In the following section, we discuss the mechanical properties of elastomer-particle assemblies in the two-dimensional packing state.

4.2 Elastomer microparticle monolayer

As well as hydrogel microparticles, the structural changes in the arrangement of fluorescence-labeled elastomer microparticles under compression at the air–water interface were clearly captured. In our previous report,[97] we observed that elastomer microparticles spaced on the air–water interface gradually approach each other upon compressing the air–water interface. When the particles are in contact with each other, a sudden increase in surface pressure (π) can be observed and a free-standing film consisting of a monolayer particle film is formed (Fig. 13(a) and (b)) that can be examined by AFM upon pulling the solid substrate up from the air–water interface. AFM observations showed that the LB films pulled up at higher surface pressure were more densely packed with particles (Fig. 13(c)). The Young's modulus of the monolayer-particle-film surface, measured by AFM indentation by tip on the cantilever, was found to correlate with the particle-packing density of the monolayer-particle film (Fig. 13(c) and (d)). The two-dimensional monolayer-particle film formed *via* particle compaction at the air–water interface is equivalent to a structure from which information in the height direction is eliminated. As a result, it became possible to discuss the properties based on a well-defined particle-array structure.[77]

Despite this pioneering study on monolayer particle films composed of elastomers, the mechanism of structural changes from particle compaction to polymer-chain diffusion has not been clearly understood for more than 35 years.[128] Further work on the diversification of the properties and the arrangement of single particles to reveal the origin of the film toughness on two dimensions is currently underway in our laboratory.

5. Material recycling of nano/microparticle-based polymers

As mentioned in the introduction, nanoparticle-based materials-recycling methods offer a unique alternative for materials recycling.[75] In this section, the materials recycling of tough

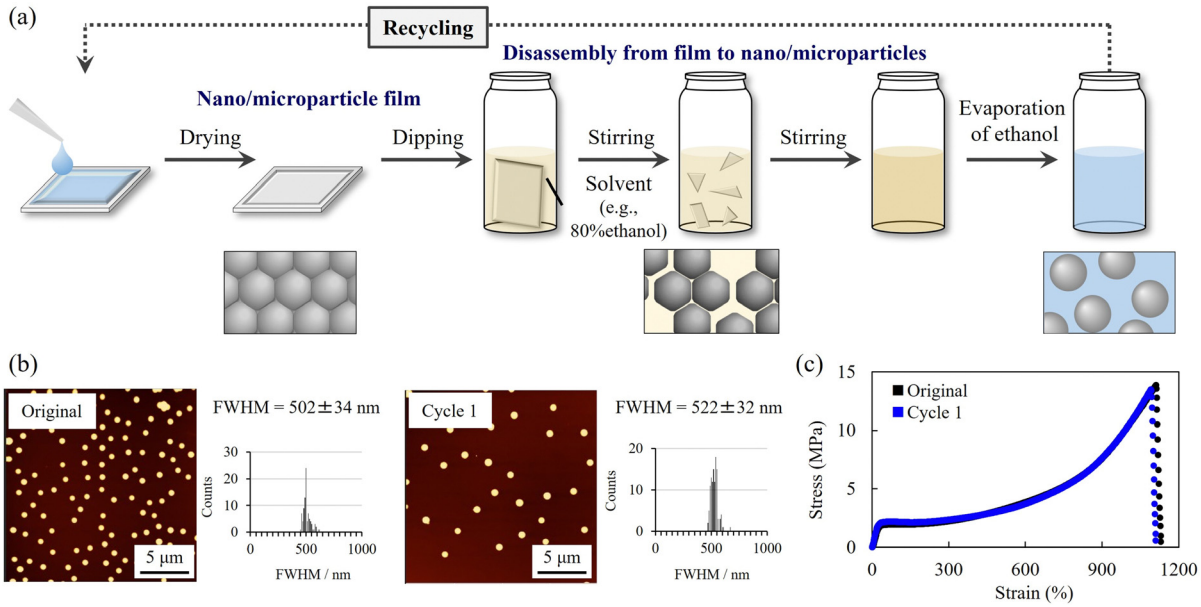

Fig. 14 (a) Schematic illustration of materials recycling using polymer nano/microparticles. In a good solvent of the polymer nano/microparticles, the films are degraded to single nano/microparticles. After removing the good solvent, aqueous pMA dispersions are obtained again. (b) AFM height images of pMA nano/microparticles before and after recycling. (c) Stress–strain curves of pMA particle-based films before (original) and after recycling (cycle 1). Adapted with permission from ref. 75 (copyright 2023 Royal Society of Chemistry).

nano/microparticle-based films, the separation of functional additives, and a recent study on the clarification of the driving force and kinetics of the recycling process are discussed.

5.1 Closed-loop recycling of nano/microparticle-based polymers

As shown in Fig. 14(a), pMA nano/microparticle-based films can be disassembled and degraded to single nano/microparticles by adding a good solvent for the pMA nano/microparticles (*e.g.*, 80% ethanol in water) at ambient temperature.[75] This disassembling into single nano/microparticles is attributed to the disentanglement of polymer chains by solvent swelling. Solvents with a lower boiling point than that of water could be easily removed *via* distillation. After an aqueous particle-containing dispersion is obtained, the films re-form upon drying the dispersions. The size, morphology, nano/microparticle chemical structure, and the fracture energy of the nano/microparticle films after recycling remain virtually unchanged (Fig. 14(b) and (c)), suggesting that chemical and physical deterioration does not occur after repeated recycling (closed-loop recycling). In addition to pMA, other tough rotaxane-crosslinked acrylate polymers can be recycled.

Considering the mechanism of film disassembling into individual nano/microparticles, this nano/microparticle-based recycling concept constitutes a groundbreaking approach that cannot be categorized as either chemical or materials recycling. Extending the scope of the nano/microparticle-based recycling strategy to other polymer materials can be expected to increase its utility.

5.2 Separation of functional additives from nano/microparticle-based films

The separation of functional additives has also been investigated. Silica, a widely used functional additive, is often used as a filler for hardening, while inorganic pigments are often used for colorization. The assembling–disassembling of a pigment-containing pMA nanoparticle-based film is shown in Fig. 15. The composite film is formed by drying a mixture of a pMA dispersion and an inorganic particle dispersion. After use, this composite film can be disassembled by immersing it in a good solvent. Then, the inorganic additives can be removed by centrifugation using the difference of density relative to the pMA particles. After removal of the inorganic pigments, the properties of the discolored films remain almost identical to those of the original pure pMA films.

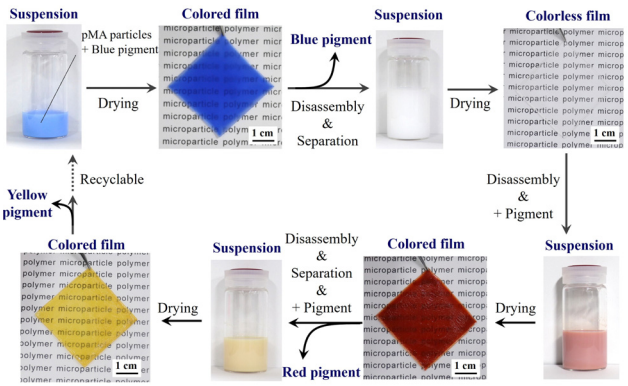

Fig. 15 Photographs of dispersions and films prepared by drying dispersions. As additives, blue, red, and yellow pigments were mixed with a pMA nano/microparticle-containing dispersion and then separated by centrifugation in a good solvent for the pMA nano/microparticles. Adapted with permission from ref. 75 (copyright 2023 Royal Society of Chemistry).

Generally, composite materials are prepared to improve the properties or functions of the individual components. However, in terms of recycling, these additives must be removed. This nano/microparticle-based separating/recycling method using silica and inorganic pigments provides a promising approach for simple waste processing.

6. Conclusions and outlook

This feature article describes the improvement of the mechanical properties of polymers prepared from aqueous polymer nano/microparticles. While first, tough nano/microparticles were obtained from introducing rotaxane as a molecular machine, a pMA nano/microparticle-based film with high toughness has recently been obtained without using rotaxanes, which provides a breakthrough for conventional waterborne latex films that are generally brittle. Furthermore, the relevance of determining the nanostructures of single particles and particle films using multiscale analysis in order to elucidate the toughening mechanism of nano/microparticle-based films was reviewed. AFM and SAXS methods can be used to determine that the deformation of nano/microparticles is correlated with the mechanical properties of films under deformation. To evaluate the particle arrays, particle monolayers were formed at the air–water interface, which enabled the visualization of the deformation and mechanical properties of single particles. In the context of problems relating to plastics, such as plastic waste, ocean pollution, and exhaustion of fossil fuels, undesirable degradation of these nano/microparticle-based materials should be avoided. In this context, we have developed a closed-loop recycling method in which the nano/microparticle-based films are disassembled into nano/microparticles simply by adding solvents, demonstrating the toughness (mechanical stability) and degradability of the films. To improve this concept, an expansion to other polymer materials can be expected to pave the way toward a more sustainable society.

Author contributions

Yuma Sasaki: original manuscript draft; Yuichiro Nishizawa: original manuscript draft; Takuma Kureha: original manuscript draft; Daisuke Suzuki: conceptualization, resources, funding acquisition, project administration, writing, review, and editing of the original manuscript draft.

Data availability

The data that support the findings of this study are available from the corresponding author upon reasonable request.

Conflicts of interest

There are no conflicts to declare.

Acknowledgements

D. S. acknowledges a CREST Grant-in Aid (JPMJCR21L2) from the Japan Science and Technology Agency (JST). The authors gratefully acknowledge all collaborators.

References

1 L. A. Felton and J. W. McGinity, *Eur. J. Pharm. Biopharm.*, 1999, **47**, 3–14.
2 N. Saito, Y. Kagari and M. Okubo, *Langmuir*, 2006, **22**, 9397–9402.
3 D. Suzuki, K. Horigome, T. Kureha, S. Matsui and T. Watanabe, *Polym. J.*, 2017, **49**, 695–702.
4 H. Minami, *Langmuir*, 2020, **36**, 8668–8679.
5 D. Suzuki, *Langmuir*, 2023, **39**, 7525–7529.
6 Y. Kitayama, S. Takigawa, E. Yuba and A. Harada, *Biomacromolecules*, 2024, **25**, 6465–6473.
7 H. Kawaguchi, *Prog. Polym. Sci.*, 2000, **25**, 1171–1210.
8 H. Ayame, N. Morimoto and K. Akiyoshi, *Bioconjugate Chem.*, 2008, **19**, 882–890.
9 Y. Hoshino, T. Kodama, Y. Okahata and K. J. Shea, *J. Am. Chem. Soc.*, 2008, **130**, 15242–15243.
10 A. C. Brown, S. E. Stabenfeldt, B. Ahn, R. T. Hannan, K. S. Dhada, E. S. Herman, V. Stefanelli, N. Guzzetta, A. Alexeev, W. A. Lam, L. A. Lyon and T. H. Barker, *Nat. Mater.*, 2014, **13**, 1108–1114.
11 T. Kureha, Y. Nagase and D. Suzuki, *ACS Omega*, 2018, **3**, 6158–6165.
12 T. Okubo, D. Suzuki, T. Yamagata, K. Horigome, K. Shibata and A. Tsuchida, *Colloid Polym. Sci.*, 2011, **289**, 1273–1281.
13 D. Suzuki, T. Yamagata, K. Horigome, K. Shibata, A. Tsuchida and T. Okubo, *Colloid Polym. Sci.*, 2012, **290**, 107–117.
14 M. Kohri, *Polym. J.*, 2019, **51**, 1127–1135.
15 E. C. Cho, J. W. Kim, A. Fernandez-Nieves and D. A. Weitz, *Nano Lett.*, 2008, **8**, 168–172.
16 D. Suzuki, T. Kobayashi, R. Yoshida and T. Hirai, *Soft Matter*, 2012, **8**, 11447–11449.
17 S. Kawahara, *Polym. J.*, 2023, **55**, 1007–1021.
18 J. Geurts, J. Bouman and A. Overbeek, *J. Coat. Technol. Res.*, 2008, **5**, 57–63.
19 M. Schulz and J. L. Keddie, *Soft Matter*, 2018, **14**, 6181–6197.
20 L. Bai, Z. Y. Xie, W. Wang, C. W. Yuan, Y. J. Zhao, Z. D. Mu, Q. F. Zhong and Z. Z. Gu, *ACS Nano*, 2014, **8**, 11094–11100.
21 Z. J. Zeng, J. H. Liang, R. H. Yu, J. H. Liu, M. W. Cao, S. J. Wang and Y. Q. Xia, *ACS Appl. Mater. Interfaces*, 2021, **13**, 25563–25570.
22 M. K. Hasan, K. Enomoto, M. Kikuchi, A. Narumi, S. Takahashi and S. Kawaguchi, *Polym. J.*, 2023, **55**, 607–616.
23 C. Fang, Q. M. Yan, Z. Z. Liu, Y. F. Lu and Z. X. Lin, *Int. J. Adhes. Adhes.*, 2018, **84**, 387–393.
24 T. Ito, C. Katsura, H. Sugimoto, E. Nakanishi and K. Inomata, *Langmuir*, 2013, **29**, 13951–13957.
25 Y. N. Zhang, Y. F. Gao, W. S. P. Carvalho, C. H. Fang and M. J. Serpe, *ACS Appl. Mater. Interfaces*, 2020, **12**, 19062–19068.
26 S. Jiang, A. Van Dyk, A. Maurice, J. Bohling, D. Fasano and S. Brownell, *Chem. Soc. Rev.*, 2017, **46**, 3792–3807.
27 B. C. McDonald, J. A. de Gouw, J. B. Gilman, S. H. Jathar, A. Akherati, C. D. Cappa, J. L. Jimenez, J. Lee-Taylor, P. L. Hayes, S. A. McKeen, Y. Y. Cui, S. W. Kim, D. R. Gentner, G. Isaacman-VanWertz, A. H. Goldstein, R. A. Harley, G. J. Frost, J. M. Roberts, T. B. Ryerson and M. Trainer, *Science*, 2018, **359**, 760–764.
28 G. L. Brown, *J. Polym. Sci.*, 1956, **22**, 423–434.
29 P. R. Sperry, B. S. Snyder, M. L. Odowd and P. M. Lesko, *Langmuir*, 1994, **10**, 2619–2628.
30 D. Sheetz, *J. Appl. Polym. Sci.*, 1965, **9**, 3759–3773.
31 P. G. De Gennes, *C. R. Seances Acad. Sci., Ser. B*, 1980, **291**, 219–221.
32 M. Joanicot, K. Wong and B. Cabane, *Macromolecules*, 1996, **29**, 4976–4984.
33 A. Du Chesne, A. Bojkova, J. Gapinski, D. Seip and P. Fischer, *J. Colloid Interface Sci.*, 2000, **224**, 91–98.
34 J. L. Keddie, *Mater. Sci. Eng., R*, 1997, **21**, 101–170.
35 M. A. Winnik, *Curr. Opin. Colloid Interface Sci.*, 1997, **2**, 192–199.
36 P. A. Steward, J. Hearn and M. C. Wilkinson, *Adv. Colloid Interface Sci.*, 2000, **86**, 195–267.

37 M. Aguirre, N. Ballard, E. Gonzalez, S. Hamzehlou, H. Sardon, M. Calderon, M. Paulis, R. Tomovska, D. Dupin, R. H. Bean, T. E. Long, J. R. Leiza and J. M. Asua, *Macromolecules*, 2023, **56**, 2579–2607.
38 L. Hughes and G. L. Brown, *J. Appl. Polym. Sci.*, 1961, **5**, 580–588.
39 H. H. Pham, J. P. S. Farinha and M. A. Winnik, *Macromolecules*, 2000, **33**, 5850–5862.
40 M. Fujii and Y. Otsuka, *Chem. High Polym.*, 1959, **16**, 484–490.
41 S. Hiroshige, H. Minato, Y. Nishizawa, Y. Sasaki, T. Kureha, M. Shibayama, K. Uenishi, T. Takata and D. Suzuki, *Polym. J.*, 2021, **53**, 345–353.
42 A. Zosel and G. Ley, *Macromolecules*, 1993, **26**, 2222–2227.
43 A. Aradian, E. Raphaël and P. G. de Gennes, *Macromolecules*, 2002, **35**, 4036–4043.
44 Y. Wang, D. Juhue, M. A. Winnik, O. M. Leung and M. C. Goh, *Langmuir*, 1992, **8**, 760–762.
45 O. Pekcan, M. A. Winnik and M. D. Croucher, *Macromolecules*, 1990, **23**, 2673–2678.
46 P. Pinenq, M. A. Winnik, B. Ernst and D. Juhué, *J. Coat. Technol.*, 2000, **72**, 47–63.
47 S. S. Hu, J. Rieger, Z. Y. Yi, J. Q. Zhang, X. L. Chen, S. V. Roth, R. Gehrke and Y. F. Men, *Langmuir*, 2010, **26**, 13216–13220.
48 J. Q. Zhang, S. S. Hu, J. Rieger, S. V. Roth, R. Gehrke and Y. F. Men, *Macromolecules*, 2008, **41**, 4353–4357.
49 T. Kureha, S. Hiroshige, D. Suzuki, J. Sawada, D. Aoki, T. Takata and M. Shibayama, *Langmuir*, 2020, **36**, 4855–4862.
50 R. Dillon, L. Matheson and E. Bradford, *J. Colloid Sci.*, 1951, **6**, 108–117.
51 J. C. Gutierrezrocca and J. W. Mcginity, *Int. J. Pharm.*, 1994, **103**, 293–301.
52 J. G. Tsavalas and D. C. Sundberg, *Langmuir*, 2010, **26**, 6960–6966.
53 H. P. Brown and C. F. Gibbs, *Ind. Eng. Chem.*, 1955, **47**, 1006–1012.
54 S. T. Eckersley and B. J. Helmer, *J. Coat. Technol.*, 1997, **69**, 97–107.
55 L. W. Morgan, *J. Appl. Polym. Sci.*, 1982, **27**, 2033–2042.
56 E. Limousin, N. Ballard and J. M. Asua, *Prog. Org. Coat.*, 2019, **129**, 69–76.
57 R. Hagen, L. Salmen, O. Karlsson and B. Wesslen, *J. Appl. Polym. Sci.*, 1996, **62**, 1067–1078.
58 Y. Rharbi, F. Boue, M. Joanicot and B. Cabane, *Macromolecules*, 1996, **29**, 4346–4359.
59 E. Limousin, N. Ballard and J. M. Asua, *Polym. Chem.*, 2019, **10**, 1823–1831.
60 H. Abdeldaim, B. Reck, K. J. Roschmann and J. M. Asua, *Macromolecules*, 2023, **56**, 3304–3315.
61 A. Noomen, *Prog. Org. Coat.*, 1989, **17**, 27–39.
62 J. W. Taylor and M. A. Winnik, *J. Coat. Technol. Res.*, 2004, **1**, 163–190.
63 S. Krishnan, A. Klein, M. S. El-Aasser and E. D. Sudol, *Macromolecules*, 2003, **36**, 3511–3518.
64 Y. Chen, S. T. Jones, I. Hancox, R. Beanland, E. J. Tunnah and S. A. F. Bon, *ACS Macro Lett.*, 2012, **1**, 603–608.
65 N. Ballard, N. Jimenez and J. M. Asua, *Part. Part. Syst. Charact.*, 2024, 2400103.
66 G. L. Cencha, M. Allasia, M. C. G. Passeggi, M. L. Gugliotta and J. R. Minari, *Prog. Org. Coat.*, 2021, **159**, 106413.
67 M. Argaiz, M. Aguirre and R. Tomovska, *Polymer*, 2023, **265**, 125571.
68 S. Manroshan and A. Baharin, *J. Appl. Polym. Sci.*, 2005, **96**, 1550–1556.
69 G. J. Desroches, P. P. Gatenil, K. Nagao and R. J. Macfarlane, *J. Polym. Sci.*, 2024, **62**, 743–752.
70 J. R. Feng, E. Odrobina and M. A. Winnik, *Macromolecules*, 1998, **31**, 5290–5299.
71 R. Raiteri, H.-J. Butt, D. Beyer and S. Jonas, *Phys. Chem. Chem. Phys.*, 1999, **1**, 4881–4887.
72 S. Hiroshige, T. Kureha, D. Aoki, J. Sawada, D. Aoki, T. Takata and D. Suzuki, *Chem. – Eur. J.*, 2017, **23**, 8405–8408.
73 Y. Sasaki, Y. Nishizawa, T. Watanabe, T. Kureha, K. Uenishi, K. Nakazono, T. Takata and D. Suzuki, *Langmuir*, 2023, **39**, 9262–9272.
74 K. Namba, Y. Sasaki, Y. Kawamura, S. Yoshida, Y. Hieda, K. Fujimoto, N. Watanabe, Y. Nishizawa, T. Uchihashi and D. Suzuki, *Langmuir*, 2024, **40**, 22614–22626.
75 T. Watanabe, H. Minato, Y. Sasaki, S. Hiroshige, H. Suzuki, N. Matsuki, K. Sano, T. Wakiya, Y. Nishizawa, T. Uchihashi, T. Kureha, M. Shibayama, T. Takata and D. Suzuki, *Green Chem.*, 2023, **25**, 3418–3424.
76 Y. Nishizawa, N. Watanabe, F.-Y. Chan, C. Ganser, T. Kawasaki, Y. Sasaki, D. Suzuki and T. Uchihashi, *ACS Appl. Mater. Interfaces*, 2024, **16**, 63073–63082.
77 Y. Sasaki, Y. Nishizawa, N. Watanabe, T. Uchihashi and D. Suzuki, *Macromol. Rapid Commun.*, 2025, **46**, 2400604.
78 R. P. Sijbesma, F. H. Beijer, L. Brunsveld, B. J. B. Folmer, J. H. K. K. Hirschberg, R. F. M. Lange, J. K. L. Lowe and E. W. Meijer, *Science*, 1997, **278**, 1601–1604.
79 R. Geyer, J. R. Jambeck and K. L. Law, *Sci. Adv.*, 2017, **3**, e1700782.
80 T. Letcher, *Plastic waste and recycling: Environmental impact, societal issues, prevention, and solutions*, Academic Press, 2020.
81 M. Strokal, P. Vriend, M. P. Bak, C. Kroeze, J. van Wijnen and T. van Emmerik, *Nat. Commun.*, 2023, **14**, 4842.
82 S. A. Park, H. Jeon, H. Kim, S. H. Shin, S. Choy, D. S. Hwang, J. M. Koo, J. Jegal, S. Y. Hwang, J. Park and D. X. Oh, *Nat. Commun.*, 2019, **10**, 2601.
83 N. Singh, D. Hui, R. Singh, I. Ahuja, L. Feo and F. Fraternali, *Composites, Part B*, 2017, **115**, 409–422.
84 M. Shamsuyeva and H. J. Endres, *Compos., Part C: Open Access*, 2021, **6**, 100168.
85 M. Häußler, M. Eck, D. Rothauer and S. Mecking, *Nature*, 2021, **590**, 423–427.
86 J. P. Gong, Y. Katsuyama, T. Kurokawa and Y. Osada, *Adv. Mater.*, 2003, **15**, 1155–1158.
87 Y. Okumura and K. Ito, *Adv. Mater.*, 2001, **13**, 485–487.
88 J. Sawada, D. Aoki, S. Uchida, H. Otsuka and T. Takata, *ACS Macro Lett.*, 2015, **4**, 598–601.
89 J. Sawada, D. Aoki, M. Kuzume, K. Nakazono, H. Otsuka and T. Takata, *Polym. Chem.*, 2017, **8**, 1878–1881.
90 K. Iijima, D. Aoki, H. Otsuka and T. Takata, *Polymer*, 2017, **128**, 392–396.
91 J. Sawada, D. Aoki, H. Otsuka and T. Takata, *Angew. Chem., Int. Ed.*, 2019, **58**, 2765–2768.
92 Y. Akae, J. Sawada, K. Nakajima and T. Takata, *Angew. Chem., Int. Ed.*, 2023, **62**, e202303341.
93 Y. Lu, D. Aoki, J. Sawada, T. Kosuge, H. Sogawa, H. Otsuka and T. Takata, *Chem. Commun.*, 2020, **56**, 3361–3364.
94 J. Ugelstad, *Die Makromolekulare Chem.: Macromol. Chem. Phys.*, 1978, **179**, 815–817.
95 M. Antonietti and K. Landfester, *Prog. Polym. Sci.*, 2002, **27**, 689–757.
96 J. M. Asua, *Prog. Polym. Sci.*, 2002, **27**, 1283–1346.
97 Y. Sasaki, S. Hiroshige, M. Takizawa, Y. Nishizawa, T. Uchihashi, H. Minato and D. Suzuki, *RSC Adv.*, 2021, **11**, 14562–14567.
98 L. Goehring, W. J. Clegg and A. F. Routh, *Phys. Rev. Lett.*, 2013, **110**, 200–208.
99 E. Pérez and J. Lang, *Macromolecules*, 1999, **32**, 1626–1636.
100 T. Ando, N. Kodera, E. Takai, D. Maruyama, K. Saito and A. Toda, *Proc. Natl. Acad. Sci. U. S. A.*, 2001, **98**, 12468–12472.
101 T. Ando, T. Uchihashi and T. Fukuma, *Prog. Surf. Sci.*, 2008, **83**, 337–437.
102 S. Matsui, T. Kureha, S. Hiroshige, M. Shibata, T. Uchihashi and D. Suzuki, *Angew. Chem., Int. Ed.*, 2017, **56**, 12146–12149.
103 S. Matsui, Y. Nishizawa, T. Uchihashi and D. Suzuki, *ACS Omega*, 2018, **3**, 10836–10842.
104 S. Matsui, K. Hosho, H. Minato, T. Uchihashi and D. Suzuki, *Chem. Commun.*, 2019, **55**, 10064–10067.
105 Y. Nishizawa, S. Matsui, K. Urayama, T. Kureha, M. Shibayama, T. Uchihashi and D. Suzuki, *Angew. Chem., Int. Ed.*, 2019, **58**, 8809–8813.
106 Y. Nishizawa, H. Yokoi, T. Uchihashi and D. Suzuki, *Soft Matter*, 2023, **19**, 5068–5075.
107 H. Minato, Y. Nishizawa, T. Uchihashi and D. Suzuki, *Polym. J.*, 2020, **52**, 1137–1141.
108 Y. Nishizawa, H. Minato, T. Inui, T. Uchihashi and D. Suzuki, *Langmuir*, 2021, **37**, 151–159.
109 Y. Nishizawa, K. Honda and D. Suzuki, *Chem. Lett.*, 2021, **50**, 1226–1235.
110 K. Hahn, G. Ley, H. Schuller and R. Oberthur, *Colloid Polym. Sci.*, 1986, **264**, 1092–1096.
111 M. A. Linne, A. Klein, G. A. Miller, L. H. Sperling and G. D. Wignall, *J. Macromol. Sci., Phys.*, 1988, **B27**, 217–231.

112 O. Pekcan, M. A. Winnik, L. Egan and M. D. Croucher, *Macromolecules*, 1983, **16**, 699–702.
113 J. R. Feng, H. Pham, V. Stoeva and M. A. Winnik, *J. Polym. Sci., Part B: Polym. Phys.*, 1998, **36**, 1129–1139.
114 T. Tamai, P. Pinenq and M. A. Winnik, *Macromolecules*, 1999, **32**, 6102–6110.
115 E. Odrobina, J. R. Feng, H. H. Pham and M. A. Winnik, *Macromolecules*, 2001, **34**, 6039–6051.
116 J. C. Haley, Y. Liu, M. A. Winnik, D. Demmer, T. Haslett and W. Lau, *Rev. Sci. Instrum.*, 2007, **78**, 084101.
117 N. Dingenouts and M. Ballauff, *Langmuir*, 1999, **15**, 3283–3288.
118 Y. F. Men, J. Rieger, S. V. Roth, R. Gehrke and X. M. Kong, *Langmuir*, 2006, **22**, 8285–8288.
119 S. S. Hu, J. Rieger, Y. Q. Lai, S. V. Roth, R. Gehrke and Y. F. Men, *Macromolecules*, 2008, **41**, 5073–5076.
120 S. S. Hu, Y. F. Men, S. V. Roth, R. Gehrke and J. Rieger, *Langmuir*, 2008, **24**, 1617–1620.
121 X. L. Chen, S. Fischer and Y. F. Men, *Langmuir*, 2011, **27**, 12807–12814.
122 I. Konko, S. Guriyanova, V. Boyko, L. C. Sun, D. Liu, B. Reck and Y. F. Men, *Langmuir*, 2019, **35**, 6075–6088.
123 Y. Nishizawa, T. Watanabe, T. Noguchi, M. Takizawa, C. Song, K. Murata, H. Minato and D. Suzuki, *Chem. Commun.*, 2022, **58**, 12927–12930.
124 F. Pinaud, K. Geisel, P. Massé, B. Catargi, L. Isa, W. Richtering, V. Ravaine and V. Schmitt, *Soft Matter*, 2014, **10**, 6963–6974.
125 Y. Gerelli, F. Camerin, S. Bochenek, M. M. Schmidt, A. Maestro, W. Richtering, E. Zaccarelli and A. Scotti, *Soft Matter*, 2024, **20**, 3653–3665.
126 T. Kawamoto, K. Yanagi, Y. Nishizawa, H. Minato and D. Suzuki, *Chem. Commun.*, 2023, **59**, 13289–13292.
127 T. Kawamoto, H. Minato and D. Suzuki, *Soft Matter*, 2024, **20**, 5836–5847.
128 W. F. Schroeder, Y. Q. Liu, J. P. Tomba, M. Soleimani, W. Lau and M. A. Winnik, *Polymer*, 2011, **52**, 3984–3993.